



# Explicit impacts of harvesting on a delayed predator–prey system with Allee effect

Bidhan Bhunia<sup>1</sup> · Tapan Kumar Kar<sup>1</sup> · Papiya Debnath<sup>2</sup>

Received: 13 September 2022 / Revised: 19 March 2023 / Accepted: 20 March 2023 / Published online: 9 May 2023  
© The Author(s), under exclusive licence to Springer-Verlag GmbH Germany, part of Springer Nature 2023

## Abstract

We propose a delayed predator–prey model with the Allee effect and individual harvesting of each species. Comparatively, fewer analyses are made to explore the impacts of harvesting efforts on population fluctuation due to time delay. Thus, our focus is on whether the harvesting effort can stabilize or destabilize the model system if the unexploited system is unstable or stable, respectively. Prey and predator harvesting has different influences on the delayed system. Prey harvesting has only stabilizing effect, whereas predator harvesting has both stabilizing and destabilizing effects. In addition, for any fixed delay, both prey and predator harvesting gives harvesting-induced switching to the system. For harvesting of either species, the delay-induced switching region and switching times increase with the increase of the Allee threshold. We observe that maximum sustainable yield (MSY) does not exist for prey harvesting, but for predator harvesting, where the pre-harvested system is stable, the system moves to stable stock at the MSY level for a smaller time delay, which does not hold for a larger time delay.

**Keywords** Predator–prey · Time delay · Allee effect · Harvesting · Stability switching · MSY

## 1 Introduction

In theoretical ecology, the thrust of research areas is to understand species interaction and determine the cause of population fluctuation. Mathematical modeling is a powerful tool for describing such interactions and reasons for oscillation. Many single species and multi-species models lead the rules and sustainability of fishery management. Based on mathematical models for managing the fisheries, several tools like maximum sustainable yield (MSY) policy [1–3],

marine-protected areas (MPAs) [4, 5], maximum economic yield (MEY) policy [6], ecosystem-based fishery management [7], balancing yield and resilience [8, 9], pretty good yield (PGY) policy [10] had been developed from time to time. Some more contributions can be found in [11–15], describing the population’s persistence with a global steady state.

Environmental fluctuation, the inhuman activity of humanity, and the inherent interaction of species are the leading cause of coexisting population in a non-equilibrium state. In ecology, two things are essential to analyze the dynamical nature one is oscillations and the other is chaos. Rosenzweig-MacArthur prey-predator model may show fluctuations, but the tri-trophic food chain model experiences chaotic dynamical behavior [16–18]. This kind of oscillation and chaotic dynamical behavior makes the model more realistic with Holling-type II functional response. Tromeur and Loeuille [8], Ghosh et al. [19] showed fluctuations might be removed from the Rosenzweig-MacArthur model with the harvesting of either prey or predator harvesting. Ghosh et al. [19] also showed that the system is stable when a predator is harvested at the optimum level. Another critical study on the tri-trophic food chain model showed that top predator harvesting might cause instability of the system [20].

T. K. Kar and P. Debnath contributed equally to this work.

✉ Bidhan Bhunia  
bidhanbhunia2016@gmail.com

Tapan Kumar Kar  
tkar1117@gmail.com

Papiya Debnath  
debpapiya@gmail.com

<sup>1</sup> Department of Mathematics, Indian Institute of Engineering Science and Technology, Shibpur, Howrah, West Bengal 711103, India

<sup>2</sup> Department of Basic Science and Humanities, Techno International New Town, Rajarhat, Kolkata, West Bengal 700156, India

The Allee effect has been considered as one of the central and critical issues in population and community ecology. It is widely recognized that the Allee effect will likely increase the extinction risk in low-density populations. Because of this, the Allee effect has received more attention from ecologists and mathematicians. This effect occurs because of several environmental and biological factors, due to mate finding, [21], social dysfunction at small population sizes, inbreeding depression [22], predator avoidance of defense, and food exploitation. The researcher pays attention to the impacts of Allee's effects on the dynamics of the population over the last decades. In population dynamics, the impact of the Allee effect on stability analysis is studied by researchers from time to time. These impacts are two types: destabilizing effect [23–25] and stabilizing effect [26–32]. Gonzalez-Olivares et al. [33] considered a model to represent the impacts of prey growth by the Allee effect and Beddington-DeAngelis-type functional response. They observed that the equilibrium point might change from stable to unstable or unstable to stable. When we add the term Allee effect in a model, it may happen that the population will reach a steady state in the long run, keeping the equilibrium point stable ([34, 35]). Even though various species exhibit Allee effects, its underlying mechanism remains unclear. Because of this reason, determining which factors regulate or induce the Allee effect continues to be an important subject in the field of both theoretical and experimental research [36]. Our objective here is not to study which factor can cause the Allee effect or which species has the Allee effect but to evoke the importance of Allee dynamics and its potential consequences in population dynamical models in the presence of delay and harvesting.

Delay differential equation model is constructed as a well-accounted strategy of modeling with the activity of stage-specific for which dynamics significantly changed of population interaction. A large number of literature studies observes that incubation time, gestation period, maturation time, and reaction time as biological processes are the main reason behind the insertion of time-delay parameter in prey-predator models and other kinds of population interaction models. To make the models' dynamics much more realistic, we incorporate time delay in biological models, which may destabilize the equilibrium points and reach to limit cycle, experiencing oscillation to grow and develop the dynamics of models. Some of the initial work with insertion of time delay is studied by Freedman, and Gopalsamy [37], Nicholson [38], Hutchinson [39] in theoretical ecology. Many authors extended their studies with a time delay in biological systems [40–44]. Their contribution leads to stability of equilibrium point globally, Hopf-bifurcation occurrence, in which delay length stability will stay. Although delay uses to model with multiple interactions of species dynamics [45, 46], it is also used in epidemiology, eco-epidemiology [47–49].

Many authors have studied the time delay model in prey-predator and food chain systems. In the predator-prey system, usually, three kinds of delay are introduced: (i) at prey-specific growth, (ii) at the functional response of the predator, and (iii) at the interacting function of the predator equation. Gourley and Kuang [50] observed that delay could cause oscillations in the stage-structure prey-predator model. Ho and Ou [51] showed the stability switching on the Lotka-Volterra-type predator-prey model. Banerjee et al. [52] discussed a prey-predator model with two-delay and Allee effects. They clarified the occurrence of sub-critical Hopf-bifurcation subjected to the time delay for simultaneous appearance of predator competition and Allee factor. Anacleto and Vidal [53] find the simultaneous influence of time delays and Allee effect in a discrete delay (at logistic term) dynamical model with Holling type-II functional response. They observed that delay might cause community extinction, coexistence, and population oscillations. They also showed the direction of Hopf-bifurcation and the occurrence of stability switching around the coexisting equilibrium.

Harvesting of population components strongly influences the evolution of the dynamical system. May et al. [3] give the notion of two kinds of harvesting (a) constant yield harvesting and (b) constant effort harvesting. Huang et al. [54] studied the Leslie-Gower-type prey-predator model with the constant yield on predator species. Xiao and Jennings [55] studied a ratio-dependent prey-predator model with constant effort harvesting. Incorporation of harvesting efforts in population dynamics was also studied by Kar and Chaudhuri [56], Kar [57], Kar and Ghorai [58], Meng et al. [59] and references therein. Kar and Pahari [60] studied a predator-prey model to address the harvesting impacts on the delay model with Beddington-DeAngelis-type functional response. Martin and Ruan [61] studied predator-prey systems with delay and constant rate harvesting, showing instability, and oscillation via Hopf-bifurcation leads to switching stability due to delay. Barman and Ghosh [62] studied a predator-prey model with Holling type II functional response and individual harvesting. They showed that the increment of the time delay parameter could not conserve the system's stability. They denied the statement of Martin and Ruan [61] that a parametric condition exists for which time delay does not change the asymptotic stability behavior of the interior steady state. Also, Meng and Li [63] proposed a delayed phytoplankton and zooplankton model with the Allee effect and combined harvesting of both species. They studied the optimal harvesting policy using harvesting effort as a control parameter. They have also studied the direction of Hopf bifurcation of the system using time delay as the bifurcation parameter.

Thus from the above literature survey, we observe that for each time delay, the Allee effect and harvesting substantially impact the dynamics of interacting species. It motivates us to construct and analyze the explicit impact of harvesting on

a delayed predator–prey model with the Allee effect. Many researchers used time delay as a control parameter to study the dynamics of the delayed predator–prey system. But, the time delay is the internal criterion of the model, and the harvesting effort is an external process user can regulate this fishing effort. In ecology, the time delay can change in a very slow timescale rather than fish effort regulation. Hence harvesting effort varies in terms of invariant time delay.

Thus in this paper, we intend to address the following issues:

- i whether a predator–prey model with the Allee effect shows only stability switching caused by time delay.
- ii whether the harvesting effort can stabilize or destabilize the model system if the unexploited system is unstable or stable, respectively.
- iii whether there is any influence of the Allee threshold on prey (or predator) dynamics.
- iv whether prey or predator harvesting at the MSY level always gives a stable, steady state.

The paper is organized as follows. Section 2 is dedicated to model formulation, discussion of model dynamics, and impacts of harvesting on the delayed predator–prey system. The impact of the Allee threshold for individual exploitation is discussed. Also, the occurrence of MSY at a stable steady state is described. Section 3 provides some discussions and concluding remarks.

## 2 The model

For the purpose of responding to the issues stated in introduction section, we consider a predator–prey model with Holling type-II functional response and the Allee effect in prey species. Time delay is introduced in the growth term and is taken as the control parameter for the unexploited system.

$$\begin{aligned} \frac{dN}{dt} &= rN \left( 1 - \frac{N(t - \tau)}{k_1} \right) (N - k_2) - \frac{\alpha NP}{a + bN} \\ \frac{dP}{dt} &= \frac{\beta \alpha NP}{a + bN} - mP \end{aligned} \tag{1}$$

where  $N(t)$  and  $P(t)$ , respectively, denote the prey and predator density at time  $t$ ,  $\tau$  is the unit of time taken by newborn to become adult at the present time,  $r$  is the intrinsic growth rate of prey species,  $k_1$  is the carrying capacity of prey population,  $k_2$  is Allee threshold,  $\alpha$  is predator consumption rate,  $a$  is a half-saturation constant of prey,  $b$  is a half-saturation constant of the predator,  $\beta$  is a conversion factor, and  $m$  is the death rate of the predator.

## 2.1 Dynamical analysis

The equilibrium points of system (1) are  $(0, 0)$ ,  $(k_1, 0)$ ,  $(k_2, 0)$ ,  $(N^*, P^*)$ , where  $N^* = \frac{ma}{\beta\alpha - mb}$  and  $P^* = \frac{r}{\alpha k_1} (a + bN^*)(k_1 - N^*)(N^* - k_2)$ .

As we concern with the coexistence of both species, we derive the conditions of the existence of interior equilibrium. For the existence of coexisting equilibrium, conditions are  $\alpha\beta - mb > 0$  and  $k_2 < N^* < k_1$ .

To study the local stability of the system, we perturbed the system about  $(N^*, P^*)$ . Using the transformation  $u = N - N^*$  and  $v = P - P^*$  in (1), we get the linear system as

$$\begin{aligned} \dot{u} &= \left\{ rN^* \left( 1 - \frac{N^*}{k_1} \right) + \frac{\alpha bN^*P^*}{(a + bN^*)^2} \right\} u - \frac{\alpha N^*}{a + bN^*} v \\ &\quad - \frac{rN^*(N^* - k_2)}{k_1} u(t - \tau) \\ \dot{v} &= \frac{\beta\alpha P^*}{(a + bN^*)^2} u \end{aligned} \tag{2}$$

Above-linearized system leads to the characteristic equation as

$$\Delta(\lambda, \tau) = \lambda^2 + a_1\lambda + a_2\lambda e^{-\lambda\tau} + a_3 = 0 \tag{3}$$

where

$$\begin{aligned} a_1 &= - \left\{ rN^* \left( 1 - \frac{N^*}{k_1} \right) + \frac{\alpha bN^*P^*}{(a + bN^*)^2} \right\}, \\ a_2 &= \frac{rN^*(N^* - k_2)}{k_1}, \\ a_3 &= \frac{\alpha\alpha^2\beta N^*P^*}{(a + bN^*)^3}. \end{aligned} \tag{4}$$

If the coexisting equilibrium exists, then  $a_1 < 0$ ,  $a_2 > 0$ ,  $a_3 > 0$ .

Since Eq. (3) is a transcendental type, two cases may arise for different values of  $\tau$ , as discussed below.

### 2.1.1 Case I: $\tau = 0$

For  $\tau = 0$ , Eq. (3) becomes a quadratic equation of  $\lambda$  and takes the form

$$\lambda^2 + (a_1 + a_2)\lambda + a_3 = 0. \tag{5}$$

Solving Eq. (5), we obtain

$$\lambda = \frac{-(a_1 + a_2) \pm \sqrt{(a_1 + a_2)^2 - 4a_3}}{2}. \tag{6}$$

Now, if

(i)  $(a_1 + a_2) > 0$  and  $a_3 > 0$ , then Eq. (5) has roots with negative real part and the system becomes locally asymptotically stable.

(ii)  $(a_1 + a_2) < 0$ , then the system becomes unstable.

**2.1.2 Case II:  $\tau \neq 0$**

If  $\tau \neq 0$ , putting  $\lambda = i\omega$  in Eq. (3), we get

$$-\omega^2 + ia_1\omega + ia_2\omega e^{-i\omega\tau} + a_3 = 0. \tag{7}$$

Then separating the real and imaginary parts of Eq. (7), we obtained

$$\begin{aligned} -\omega^2 + \omega a_2 \sin(\omega\tau) + a_3 &= 0, \\ a_1\omega + a_2\omega \cos(\omega\tau) &= 0. \end{aligned} \tag{8}$$

Squaring and adding two equations of (8), we get

$$\omega^4 + (a_1^2 - a_2^2 - 2a_3)\omega^2 + a_3^2 = 0. \tag{9}$$

Equation (9) has two positive roots as

$$\omega_{\pm} = \sqrt{\frac{-(a_1^2 - a_2^2 - 2a_3) \pm \sqrt{(a_1^2 - a_2^2 - 2a_3)^2 - 4a_3^2}}{2}}, \tag{10}$$

if the conditions  $a_1^2 - a_2^2 - 2a_3 < 0$  and  $(a_1^2 - a_2^2 - 2a_3)^2 - 4a_3^2 > 0$  are satisfied.

From Eq. (8), we obtain  $\tau_n^{\pm}$  ( $n = 0, 1, 2, \dots$ ) corresponding to each  $\omega_{\pm}$  as

$$\tau_n^{\pm} = \frac{1}{\omega_{\pm}} \arccos\left(-\frac{a_1}{a_2}\right) + \frac{2n\pi}{\omega_{\pm}}, n = 0, 1, 2, 3, \dots \tag{11}$$

From these analyses, we observe that one or more pairs of eigenvalues must present for which zero real part exists at  $\tau = \tau_n^{\pm}$ . Now we will check the changing of the real part when  $\tau$  passes through  $\tau_n^{\pm}$ . The rate of change of the real part of eigenvalue at  $\tau_n^{\pm}$  is called the transversality condition.

Now,

$$\left(\frac{d(Re\lambda)}{d\tau}\right)^{-1} \Big|_{\tau=\tau_n^{\pm}} = \frac{\omega^4 - a_3^2}{\omega^2\{(\omega^2 - a_3)^2 + a_1^2\omega^2\}}$$

and

$$sign\left(\frac{d(Re\lambda)}{d\tau}\right)^{-1} \Big|_{\tau=\tau_n^{\pm}} = sign(\omega^4 - a_3^2).$$

Therefore,

$$\frac{d(Re\lambda)}{d\tau} \Big|_{\tau_n^+} > 0$$

and

$$\frac{d(Re\lambda)}{d\tau} \Big|_{\tau_n^-} < 0.$$

These two conditions tell us that if the real part of any eigenvalue is zero either at  $\tau_n^+$  and  $\tau_n^-$ , then the real part of eigenvalues becomes positive and negative when  $\tau$  increases toward  $\tau_n^+$  and  $\tau_n^-$ , respectively, and thus Hopf-bifurcation occurs at  $\tau_n^{\pm}$ .

Now we want to find the number of eigenvalues that crosses the imaginary axis of  $\lambda$ . For this purpose, we will prove the following lemma.

**Lemma 1** *The characteristic equation  $F(\lambda, \tau) = \lambda^2 + a_1\lambda + a_2\lambda e^{-\lambda\tau} + a_3 = 0$ , where  $a_1 < 0, a_2 > 0$ , and  $a_3 > 0$ , has simple roots on the imaginary axis.*

**Proof** If possible let  $\lambda = i\omega$  is the root of  $F(\lambda, \tau) = 0$  and all roots are not simple. So  $\frac{\partial F}{\partial \lambda} \Big|_{\lambda=i\omega} = 0$  i.e.,  $2\lambda + a_1 + a_2e^{-\lambda\tau}(1 - \lambda\tau) = 0$ . Substituting the value of  $\lambda = i\omega$  and  $e^{-\lambda\tau}$  in  $F(\lambda, \tau) = 0$ , we obtain  $a_1 = \frac{2}{\tau} > 0$ . This leads to the contradiction of our assumption that roots are not simple. Hence the roots are simple.  $\square$

It also follows from the above lemma that the eigenvalues pairwise cross the imaginary axis at each  $\tau_n^+$  and  $\tau_n^-$ .

**Remark 1** As  $\omega_- < \omega_+, \tau_{n+1}^- - \tau_n^- = \frac{2\pi}{\omega_-} > \frac{2\pi}{\omega_+} = \tau_{n+1}^+ - \tau_n^+$  for  $n = 0, 1, 2, \dots$

The above condition shows that at least one of the  $\tau^+$  series will be less than from  $\tau^-$  series for an unharvested system.

**Theorem 1** *If  $a_1 + a_2 > 0$  and  $\tau_0^+ < \tau_1^+ < \tau_0^-$ , then the system shows stable nature in  $[0, \tau_0^+)$ , and Hopf-bifurcation occurs at  $\tau_0^+$  and unstable for all  $\tau > \tau_0^+$ .*

**Proof** Assume the condition  $a_1 + a_2 > 0$  in Eq. (3), and  $\tau_0^+ < \tau_1^+ < \tau_0^-$  holds. When there is no delay, system (2) is stable since both the eigenvalues will have a real negative part. Now if we increase the delay, then  $\lambda = i\omega_+$  will be the simple eigenvalue at  $\tau = \tau_0^+$  (see Lemma 1). Since the eigenvalues will be in the complex conjugate, there exists a pair  $\lambda = \pm i\omega_+$  at  $\tau_0^+$ .

When the transversality condition is satisfied at  $\tau = \tau_0^+$ , above-mentioned pair of eigenvalues crosses the imaginary axis and consists positive real part for increasing delay toward  $\tau_0^+$ , and the system turns unstable.

Corresponding to delay at  $\tau_1^+$ , there exists a pair of eigenvalue  $\lambda = \pm i\omega_+$ . Here the transversality condition at  $\tau = \tau_1^+$  suggests that these eigenvalues cross the imaginary axis pairwise. Thus, when the delay is greater than  $\tau_1^+$ , the pair of eigenvalues have the positive real part, so the system becomes unstable.

As discussed above, a pair of eigenvalue  $\lambda = \pm i\omega_-$  exists at  $\tau_0^-$ . Due to the transversality condition, the pair of eigenvalues cross the imaginary axis, and the real part becomes negative. However, the eigenvalues stay with a positive real part when increasing delay passes through  $\tau = \tau_1^+$  and instability occurs.

At every  $\tau_n^+$  or  $\tau_n^-$ , the imaginary axis is crossed by only one pair of eigenvalues, and there is no possibility of occurrence of two successive  $\tau_n^-$  (see Remark 1); instability always occurs for delay  $\tau > \tau_0^+$ .  $\square$

**Example 2.1** Now taking parameter set as:  $r = 0.007, k_1 = 157, k_2 = 5, a = 9, b = 0.007, m = 0.13, \alpha = 0.6, \beta = 0.02$  in system (1), the interior steady state of the system becomes (105.50, 3.74). Here the values of  $\tau_0^+ = 2.17, \tau_1^+ = 15.95$  and  $\tau_0^- = 16.26$ . It is observed that the system is stable for  $\tau \in [0, 2.17)$  and unstable for all  $\tau > 2.17$ .

**Theorem 2** If  $a_1 + a_2 > 0$  and  $0 < \tau_0^+ < \tau_0^- < \tau_1^+ < \tau_1^- < \dots < \tau_k^+ < \tau_{k+1}^+ < \tau_k^- < \dots$  for some  $k \in \mathbb{Z}^+$ , then switching occurs in  $k$  times from stable to unstable, then stable and finally for  $\tau > \tau_k^+$  system moves to unstable state. Also at  $\tau = \tau_n^\pm$ , Hopf-bifurcation occurs.

**Proof** Let us first consider three orders in given inequality  $\tau_0^+ < \tau_0^- < \tau_1^+$ , where  $\tau_0^+, \tau_0^-$  and  $\tau_1^+$  are the Hopf-Bifurcation points. The system exhibits stable behavior at  $\tau = 0$  since the real part of the eigenvalue is negative. When delay is increased, a pair of purely imaginary roots  $\lambda = \pm i\omega_+$  of (5) exists at  $\tau_0^+$ . At  $\tau_0^+$ , the transversality condition determines the positive real part of the eigenvalues appeared for the pair mentioned above with increasing delay through  $\tau_0^+$ . So, the system will no longer persist in a stable state. Again for increasing  $\tau$ , there corresponds to a purely imaginary root at  $\tau_0^-$ . The transversality condition at  $\tau_0^-$  suggests two eigenvalues with positive real part, which possess purely imaginary eigenvalue at  $\tau_0^-$ . But it has a negative real part when  $\tau$  crosses  $\tau_0^-$ . This leads to the stability of the model. So, stability switching occurs (i.e., stable to unstable and then stable) at the positive equilibrium of system (1) with increasing delay.

Likewise, for every other  $\tau \leq \tau_k^-$ , the stability switching will be continued  $\tau < \tau_k^+$ , and the number of switching is  $k$ . If the delay parameter satisfies  $\tau_k^+ < \tau_{k+1}^+ < \tau_k^-$ , the arguments in Theorem 1 tell that the system is always unstable for  $\tau > \tau_k^+$ .  $\square$

**Example 2.2** Now we consider the parameter set as:  $r = 0.005, k_1 = 150, k_2 = 5, a = 9, b = 0.002, \alpha = 0.7, \beta = 0.02, m = 0.12$  in model (1). Then coexisting equilibrium (78.49, 2.29) of the non-delayed system is asymptotically stable. When  $\tau$  increases, the system experiences five stability switching from stable to unstable and then stable, and there exists  $\tau_5^+$  such that the system becomes unstable for

all  $\tau > \tau_5^+$ . The delays  $\tau_n^\pm$ , (for  $n = 0, 1, 2, \dots, 5$ ) are given below.

$\tau_0^+ = 0.95$	$\tau_0^- = 1.15$
$\tau_1^+ = 40.50$	$\tau_1^- = 49.47$
$\tau_2^+ = 80.05$	$\tau_2^- = 97.78$
$\tau_3^+ = 119.60$	$\tau_3^- = 146.09$
$\tau_4^+ = 159.16$	$\tau_4^- = 194.40$
$\tau_5^+ = 198.71$	$\tau_5^- = 242.71$
$\tau_6^+ = 238.26$	

From the above explanation, we can state that system (1) becomes stable for  $\tau \in (0, \tau_0^+) \cup (\tau_0^-, \tau_1^+) \cup (\tau_1^-, \tau_2^+) \cup (\tau_2^-, \tau_3^+) \cup (\tau_3^-, \tau_4^+) \cup (\tau_4^-, \tau_5^+)$ , and unstable for  $\tau \in (\tau_0^+, \tau_0^-) \cup (\tau_1^+, \tau_1^-) \cup (\tau_2^+, \tau_2^-) \cup (\tau_3^+, \tau_3^-) \cup (\tau_4^+, \tau_4^-) \cup (\tau_5^+, \infty)$ , and experiences Hopf-bifurcation at  $\tau = \tau_n^\pm$ , ( $n = 0, 1, 2, \dots, 5$ ).

**The impacts of Allee threshold**

The Allee threshold has different influences on dynamic system (1). Due to the change of Allee threshold  $k_2$ , the equilibrium component of  $(N^*, P^*)$ , the positive roots  $\omega_\pm$ , and the corresponding  $\tau_n^\pm$  are changed. It is given as follows:

Let us consider  $K = \frac{-(a_1^2 - a_2^2 - 2a_3)}{\sqrt{(a_1^2 - a_2^2 - 2a_3)^2 - 4a_3^2}}$  and  $z = \frac{-a_1}{a_2^2 \sqrt{1 - (\frac{a_1}{a_2})^2}}$  which are positive, since  $a_1^2 - a_2^2 - 2a_3 < 0$  and  $a_1 < 0$ . We have  $\frac{da_2}{dk_2} < 0$  (from (4)).

Now,

$$\begin{aligned} \frac{d\omega_+}{dk_2} &= \frac{a_2}{2\omega_+} (1 + K) \frac{da_2}{dk_2} < 0, \\ \frac{d\omega_-}{dk_2} &= \frac{a_2}{2\omega_-} (1 - K) \frac{da_2}{dk_2} <, =, \text{ or } > 0 \text{ according as} \\ &K <, =, \text{ or } > 1, \\ \frac{d\tau_n^+}{dk_2} &= \frac{1}{\omega_+} \left[ z + \frac{a_2}{2} (\arccos(-a_1/a_2) + 2n\pi)(1 + K) \right] \\ \frac{da_2}{dk_2} &< 0, \\ \frac{d\tau_n^-}{dk_2} &= \frac{1}{\omega_-} \left[ z + \frac{a_2}{2} (\arccos(-a_1/a_2) + 2n\pi)(1 - K) \right] \\ \times \frac{da_2}{dk_2} &\begin{cases} < 0, & \text{if } K < 1 \\ > 0, & \text{if } z + \frac{a_2}{2} (\arccos(-a_1/a_2) + 2n\pi)(1 - K) < 0 \end{cases} \end{aligned}$$

Thus, from the above conditions, we can say that  $\omega_+$  and  $\tau_n^+$  will always decrease with the Allee threshold. But, the increase or decrease of  $\omega_-$  and  $\tau_n^-$  depends on the conditions as given above.

## 2.2 Harvesting impacts on delay model

Harvesting has a strong impact on the dynamics of any ecological system of interacting species. Depending on the harvesting strategy on different trophic level, the long-run stationary biomass of the coexisting population may be unstable and ultimately goes to extinction. But most of the ecological models of interacting species with time delay are analyzed, taking delay as a control parameter. Being time delay is an inherent factor and changes on a very slow timescale, especially for harvested systems, we should consider harvesting effort as a control parameter to regulate the system. We will study the harvesting impacts on the delay system with this motivation.

### 2.2.1 Prey harvesting

Considering the harvesting of prey species, the model becomes

$$\begin{aligned} \frac{dN}{dt} &= rN \left( 1 - \frac{N(t-\tau)}{k_1} \right) (N - k_2) - \frac{\alpha NP}{a + bN} - E_1 N \\ \frac{dP}{dt} &= \frac{\beta \alpha NP}{a + bN} - mP \end{aligned} \tag{12}$$

where  $E_1$  is the harvesting effort of the prey species.

The steady states are  $(0, 0)$ ,  $(N^*, P^*)$  where  $N^* = \frac{ma}{\alpha\beta - mb}$ ,  $P^* = \frac{(a+bN^*)}{\alpha} \left\{ \frac{r}{k_1} (k_1 - N^*) (N^* - k_2) - E_1 \right\}$ .

Now  $(N^*, P^*)$  exists if  $\alpha\beta - mb > 0$  and  $0 < E_1 < \frac{r}{k_1} (k_1 - N^*) (N^* - k_2)$ .

Linearize system about the equilibrium point becomes

$$\begin{aligned} \dot{u} &= \left\{ rN^* \left( 1 - \frac{N^*}{k_1} \right) + \frac{\alpha b N^* P^*}{(a + bN^*)^2} \right\} u - \frac{\alpha N^*}{a + bN^*} v \\ &\quad - \frac{rN^*(N^* - k_2)}{k_1} u(t - \tau) \\ \dot{v} &= \frac{\beta \alpha P^*}{(a + bN^*)^2} u. \end{aligned} \tag{13}$$

Considering

$$\begin{aligned} a_1 &= - \left\{ rN^* \left( 1 - \frac{N^*}{k_1} \right) + \frac{\alpha b N^* P^*}{(a + bN^*)^2} \right\}, \\ a_2 &= \frac{rN^*(N^* - k_2)}{k_1}, \\ a_3 &= \frac{\alpha \alpha^2 \beta N^* P^*}{(a + bN^*)^3}, \end{aligned} \tag{14}$$

we get

$$\omega_{\pm}(E_1) = \sqrt{\frac{-(a_1^2 - a_2^2 - 2a_3) \pm \sqrt{(a_1^2 - a_2^2 - 2a_3)^2 - 4a_3^2}}{2}}, \tag{15}$$

if the conditions  $a_1^2 - a_2^2 - 2a_3 < 0$  and  $(a_1^2 - a_2^2 - 2a_3)^2 - 4a_3^2 > 0$  are satisfied,

$$\tau_n^{\pm}(E_1) = \frac{1}{\omega_{\pm}} \arccos \left( -\frac{a_1}{a_2} \right) + \frac{2n\pi}{\omega_{\pm}}, n = 0, 1, 2, 3, \dots \tag{16}$$

**Theorem 3** *If  $\tau_n^+(E_1)$  is increasing function of effort and unharvested system (1) incorporates delay  $T$  in the range  $(0, \tau_0^+(0))$ , then harvesting of prey species cannot effect the stability of the model system.*

**Proof** Let  $\tau_n^+(E_1)$  is an increasing function of harvesting effort. If we consider a delay  $T \in (0, \tau_0^+(0))$ , the system remains stable. Since  $\tau_0^+(E_1)$  is increasing function with increasing harvesting effort  $E_1$ ,  $T \in (0, \tau_0^+(0)) \subseteq (0, \tau_0^+(E_1))$ . Thus, harvesting effort cannot break the stability nature of the system.  $\square$

Now if we take a parameter set satisfying the condition  $\tau_0^+(0) < \tau_1^+(0) < \tau_0^-(0)$ , then the system cannot experience stability switching. So we may state that delay is the cause of instability of the unharvested system. The above description gives a clear notion that for the delay  $T \in (0, \tau_0^+(0))$ , prey harvesting does not affect its stability. So we need to study the stability behavior for delay exceeding  $\tau_0^+(0)$  due to harvest. The related results are stated in the following theorem.

**Theorem 4** *If  $\tau_n^+(E_1)$  is an increasing function, then for the above parametric restrictions, two cases arise as follows:*

(i) *If the delay  $T \in (\tau_0^+(0), \tau_{max})$ , the instability of the system can be removed with an appropriate harvesting effort, and further increase of effort keeps the system stable. Here  $\tau_{max} = \lim_{E_1 \rightarrow E^*} \tau_0^+(E_1)$  and  $E^* = \frac{r}{k_1} (k_1 - N^*) (N^* - k_2)$ , where  $N^* = \frac{ma}{\alpha\beta - mb}$ .*

(ii) *If the delay  $T > \tau_{max}$ , any harvesting effort cannot stabilize the system.*

**Proof** (i) When population of prey species is subject to harvesting, system shows stability for every  $(E_1, T) \in (0, E^*) \times (0, \tau_0^+(E_1))$  and instability for  $(E_1, T) \in (0, E^*) \times (\tau_0^+(E_1), \infty)$ . Now, consider the delay  $T \in (\tau_0^+(E_1), \tau_{max})$ . As  $\tau_0^+(E_1)$  increases with increasing effort  $E_1$ , the coordinate  $(E_1, T)$  in the region  $(0, E_1) \times (\tau_0^+(E_1), \tau_{max})$ , may move to the region  $(0, E^*) \times (0, \tau_0^+(E_1))$ , for any small

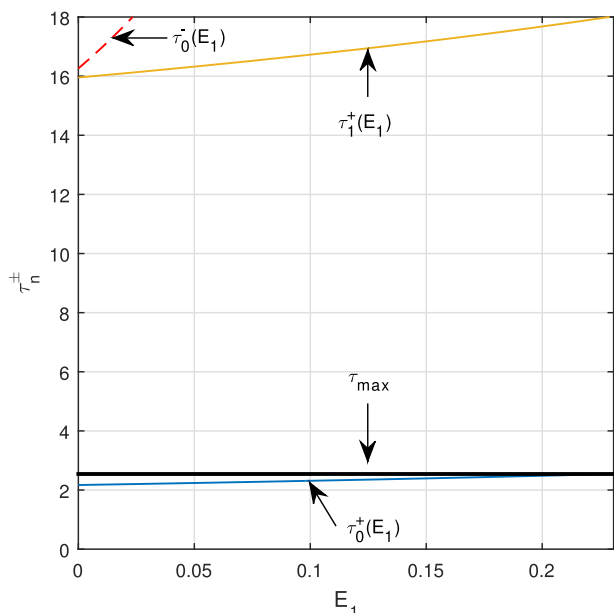


**Fig. 1** Depicted increasing effort curves  $\tau = \tau_n^\pm(E_1)$ . Stability region shown in  $E_1 - \tau_n^\pm$  plane with respect to harvesting effort

change of effort, beyond the critical level (i.e., the effort for which just cross the curve  $\tau = \tau_0^+(E_1)$ ). Thus the system has a stable state.

(ii) If we consider delay  $T > \tau_{max}$ , then the arbitrary co-ordinate cannot enter into the region  $(0, E^*) \times (0, \tau_0^+(E_1))$  by changing harvesting effort. Thus the system stays unstable state for any effort. □

Consider the parameter set as in Example. 2.1. For the existence of interior equilibrium, effort must lie in the range  $(0, 0.23)$ . The horizontal black line specifies  $\tau = \tau_{max}$ . The red dashed curves are plotted for  $\tau = \tau_0^-(E_1)$  in Fig. 1. Remaining solid curves represent  $\tau = \tau_0^+(E_1), \tau = \tau_1^+(E_1)$ . The region enclosed by  $\tau = \tau_0^+(E_1)$  and  $E_1$ -axis is the stability region, and the whole region after  $\tau = \tau_0^+(E_1)$  is the instability region. It is seen that if  $T$  lies in the interval  $(0, \tau_0^+(0))$ , then the coordinate  $(E_1, T)$  always be in the region of stability for any effort  $E_1$  lies in  $(0, 0.23)$  (as Theorem 3). Here  $\tau_{max} = 2.54$ . It is seen that for  $T \in (\tau_0^+(0), \tau_{max})$ , the co-ordinate  $(E_1, T)$  lies in the unstable region bounded by  $\tau = \tau_0^+(E_1)$  and  $\tau = \tau_{max}$  for a smaller effort level. However the co-ordinate enters into the stability region for increasing effort as stated in Theorem 4(i) and for  $T > \tau_{max}$ , the point  $(E_1, T)$  lies in the unstable region for all possible harvesting effort as stated in Theorem 4(ii).

This analysis states that when the system is harvested, it cannot change stable behavior if the unharvested system is stable. Also, when the delay is more significant than  $\tau_{max}$  (i.e.,  $T > \tau_{max}$ ), prey harvesting cannot change the instability behavior. But, when the delay is of moderate length

(i.e.,  $\tau_0^+(0) < T < \tau_{max}$ ), the system becomes stable when the effort crosses the critical level, i.e., the effort for which coordinate  $(E_1, T)$  moves from unstable to stable region.

Now we will seek the effect of harvesting when an unharvested system leads to stability switching. We set the parameters as in example 2.2 for system (12). We show that there are having five stability switching (stable to the unstable region then back to stable region) due to delay of the unharvested system. The system becomes unstable if we increase the delay after five stability switches (see example 2.2). The equilibrium will coexist if the effort  $E_1$  is in the range  $(0, 0.17)$ . Like previous analysis different curves  $\tau = \tau_n^\pm(E_1)$  are shown in Fig. 2.

The dashed and solid curves in Fig. 2, respectively, represent  $\tau = \tau_n^-(E_1)$  and  $\tau = \tau_n^+(E_1)$ ,  $(n = 0, 1, 2, \dots)$ . The region enclosed by first solid curve and  $E_1$ - axis is the stable region. The region between any solid curve and the next dashed curve is the instability region. The region between the dashed curve and the next solid curve is the stable region until they cut each other for increasing effort  $E_1$ . After crossing two curves, two solid curves will be appeared simultaneously. These successive appearances of two solid curves result in instability regions between the curves and the regions above the curves, in this particular range of  $E_1$ . Let  $S_1$  is the region between  $E_1$ - axis and  $\tau = \tau_0^+(E_1)$ , the region between  $\tau = \tau_n^+(E_1)$  and  $\tau = \tau_n^-(E_1)$  named as  $U_{n+1}$ , the region between  $\tau = \tau_n^-(E_1)$  and  $\tau = \tau_{n+1}^+(E_1)$  named as  $S_{n+2}(n = 0, 1, \dots)$ . We show the regions  $S_1, S_2, S_3$  are stable region and  $U_1, U_2$  are unstable region until the two  $\tau = \tau_n^+(E_1)$  and  $\tau = \tau_{n+1}^+(E_1)$  occurs successively giving the instability regions.

The following stability nature is observed in Fig. 2 for varying harvesting efforts with a fixed delay in system (12).

(a) If delay  $T \in (0, \tau_0^+(0)) = (0, 0.95)$ , the co-ordinate  $(E_1, T)$  stays in the region  $S_1$  for any harvesting effort level. Hence the system will be stable in that region.

(b) If delay  $T \in (\tau_0^+(0), \tau_0^-(0)) = (0.95, 1.15)$ , the co-ordinate  $(E_1, T)$  lies in the region  $U_1$  till the harvesting effort becomes large enough to force it for entering  $U_1$  region to  $S_1$  region. Henceforth, when the harvesting effort is large, it can remove the instability, and a simultaneous population will exist at equilibrium.

(c) If delay  $T \in (\tau_0^-(0), \tau_1^-(0)) = (1.15, 40.50)$ , the co-ordinate  $(E_1, T)$  moves from stable region  $S_2$  to unstable region  $U_1$  and then it is back to stable region  $S_1$  with the increase of harvesting effort. The coordinate enters into the region  $S_1$  when the harvesting effort is sufficiently close to maximum effort  $E^*$ . Such kind of harvesting effort shows a stable, steady state with low predator density. This kind of region shifting signifies unharvested stable system can be destabilized due to harvesting, but when effort further increases back to a stable region. Thus one stable switching arises for the increase of harvesting effort.

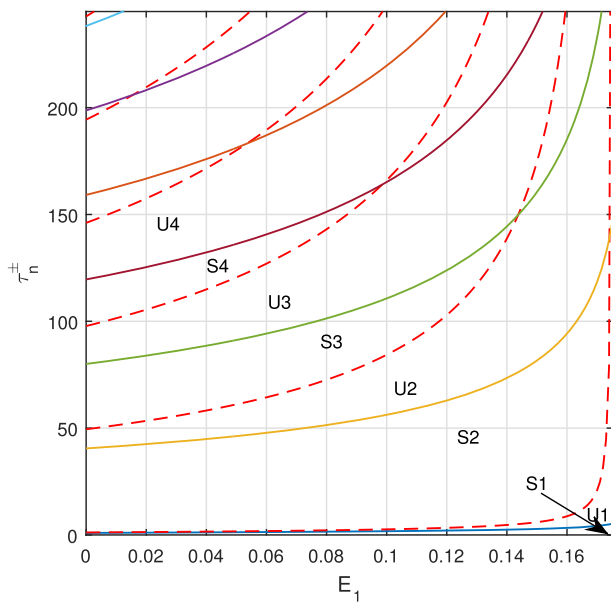


**Fig. 2** Region between  $\tau = \tau_n^+(E_1)$  (solid) curve and  $\tau = \tau_n^-(E_1)$  (dashed) curve is the stable region  $S_n$  and unstable region  $U_n$

(d) If delay  $T \in (\tau_1^+(0), \tau_1^-(0)) = (1.15, 40.50)$ , the co-ordinate  $(E_1, T)$  moves from unstable region  $U_2$  to stable region  $S_2$  and then back to unstable region  $U_1$  with the increase harvesting effort. This kind of region shifting signifies an unstable unharvested system that can be stabilized due to harvesting, but when effort further increases back to an unstable region. Thus one unstable switching arises with increasing harvesting effort.

(e) If delay  $T \in (\tau_1^-(0), \tau_2^+(0)) = (40.50, 49.47)$ , successive moving of the coordinate  $(E_1, T)$  passes through the regions  $S_3, U_2, S_2$  and  $U_1$  as the harvesting effort increases.

(f) If  $T > \tau_{max}^+(E')$  where  $E' \in (0, E^*)$ , then the system remains in unstable state for all harvesting effort. Here  $\tau_{max}^+(E')$  is the maximum of all  $\tau_k^+(E')$  for  $k \leq 5$ , the switching number of the system for every  $E_1$ . It is the case that is observed in Theorem 4(ii).

**2.2.2 Influence of Allee threshold on prey harvesting**

The Allee effect makes the dynamics more sensitive and accurate to understand the dynamical configuration better. The conditions of local stability with an analytical approach show that all are a function of the Allee threshold in prey harvesting. From Eq. (4), (10), and (11), we must say  $\tau_n^\pm = \tau_n^\pm(k_2)$ . We are considering the same parameter set as in Example 2.2 and observe the dynamical changes with the Allee threshold  $k_2 = 0.001, 2, 3, 4.5, 5, 5.5$  in Fig. 3.

When Allee threshold  $k_2$  increases (or decreases) for the above parameter set as in example 2.2, the pre-harvested system shows the following observations:

- (i) Both  $\tau_0^+$  and  $\tau_0^-$  decreases (or increases).

- (ii) Each  $\tau_n^+, n \in \mathbb{N}$  increases (or decreases) and  $\tau_n^-, n \in \mathbb{N}$  decreases (or increases).

- (iii) The length of harvesting effort decrease (or increase).

Thus, we can say that when the Allee threshold increases, then each of  $\tau_0^+$  and  $\tau_0^-$  decreases for the pre-harvested system. Also, from Fig. 3, we observe that all the curves increase when the harvesting effort range increases. It means first stable region in between  $E_1$ -axis and curves  $\tau = \tau_0^+(E_1)$  and the first unstable region enclosed by the curve  $\tau = \tau_0^+(E_1)$  and  $\tau = \tau_0^-(E_1)$  are decreased for increasing threshold. When delay change is very less, then the area of the first stable region of the system decreases for increasing the Allee threshold. In other words, when the Allee threshold is very less or closer to zero, the first stable region will be greater than the other region for different thresholds. Again when Allee threshold increases then  $\tau_n^+, n \in \mathbb{N}$  increases and  $\tau_n^-, n \in \mathbb{N}$  decreases for pre-harvested system. It means the traps between the region enclosed by  $\tau = \tau_n^-(E_1), n \in \mathbb{N} \cup \{0\}$  and  $\tau = \tau_n^+(E_1), n \in \mathbb{N}$  will decrease up to a certain value of  $E_1$  where curves cross each other. Also, the number of switching increases for increasing the Allee threshold. Since switching times increase, the system becomes more sensitive, i.e., if we choose a particular delay value and increase the effort range, then for a slight change of effort system moves from stable to unstable back to a stable region or unstable to stable back to the unstable region.

**2.2.3 Predator harvesting**

In this section, we study the impact of predator harvesting on model system (1). The model takes the form:

$$\begin{aligned} \frac{dN}{dt} &= rN \left( 1 - \frac{N(t-\tau)}{k_1} \right) (N - k_2) - \frac{\alpha NP}{a + bN} \\ \frac{dP}{dt} &= \frac{\beta \alpha NP}{a + bN} - mP - E_2 P \end{aligned} \tag{17}$$

where  $E_2$  is the harvesting effort on the predator population.

The equilibrium points are  $(0, 0), (k_1, 0), (k_2, 0), (N^*, P^*)$ ,

where  $N^* = \frac{(m+E_2)a}{\alpha\beta - (m+E_2)b}, P^* = \frac{(a+bN^*)}{\alpha} \left\{ \frac{r}{k_1} (k_1 - N^*) (N^* - k_2) \right\}$ .

Coexisting equilibrium  $(N^*, P^*)$  exists if  $E_2 < \frac{\alpha\beta}{b} - m$  and  $\frac{k_2\alpha\beta}{a+bk_2} - m < E_2 < \frac{k_1\alpha\beta}{a+bk_1} - m$ . But,  $\frac{k_1\alpha\beta}{a+bk_1} - m = \frac{\frac{\alpha\beta}{b}}{\frac{a}{bk_1} + 1} - m < \frac{\alpha\beta}{b} - m$ .

Thus, the coexistence depends only on  $\frac{k_2\alpha\beta}{a+bk_2} - m < E_2 < \frac{k_1\alpha\beta}{a+bk_1} - m$ . Since the harvesting effort cannot be negative, the conditions become  $\max\{0, \frac{k_2\alpha\beta}{a+bk_2} - m\} < E_2 < \frac{k_1\alpha\beta}{a+bk_1} - m$  and  $k_1 > \frac{ma}{\alpha\beta - mb}$ .



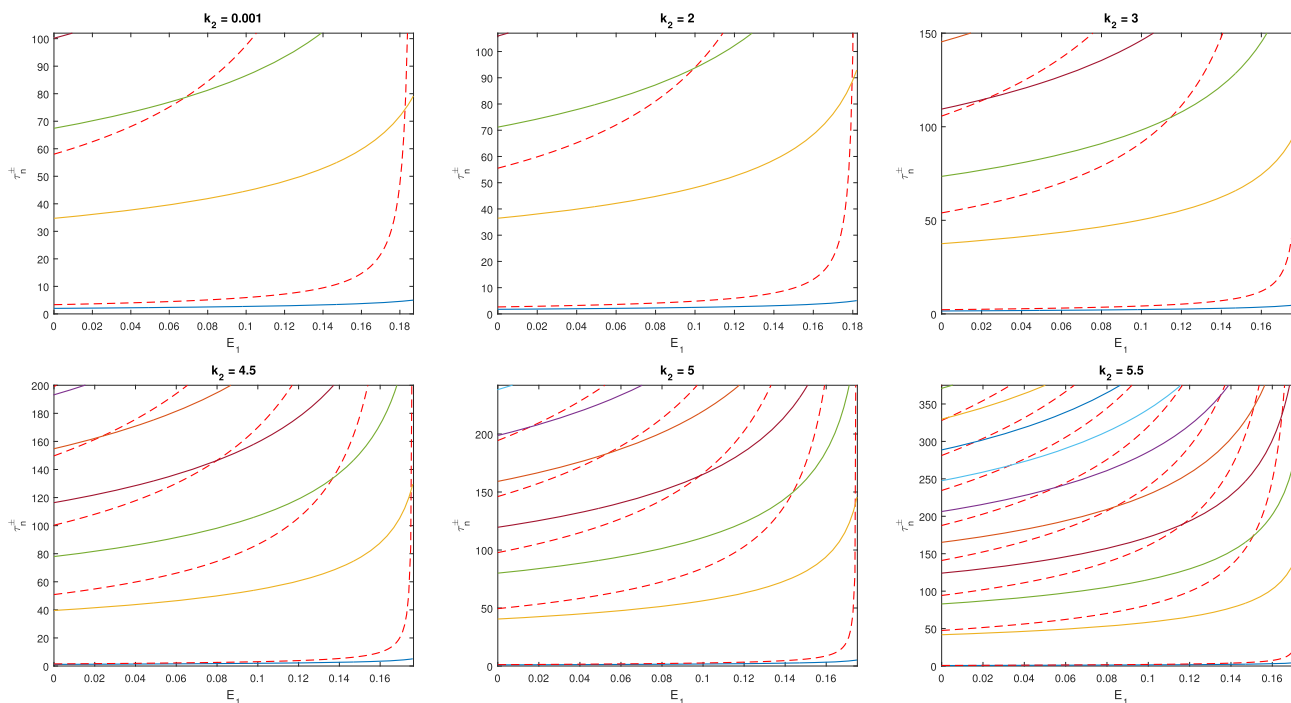


**Fig. 3** Stability switchings are shown for different Allee thresholds  $k_2 = 0.001, 2, 3, 4.5, 5, 5.5$  due to an increase in harvesting effort

The linearized form of model (17) about the coexisting equilibrium takes the form:

$$\begin{aligned} \dot{u} &= \left\{ rN^* \left( 1 - \frac{N^*}{k_1} \right) + \frac{\alpha bN^*P^*}{(a + bN)^2} \right\} u - \frac{\alpha N^*}{a + bN^*} v \\ &\quad - \frac{rN^*(N^* - k_2)}{k_1} u(t - \tau), \\ \dot{v} &= \frac{\beta \alpha a P^*}{(a + bN^*)^2} u. \end{aligned} \tag{18}$$

Assuming

$$\begin{aligned} a_1 &= - \left\{ rN^* \left( 1 - \frac{N^*}{k_1} \right) + \frac{\alpha bN^*P^*}{(a + bN)^2} \right\}, \\ a_2 &= \frac{rN^*(N^* - k_2)}{k_1}, \\ a_3 &= \frac{a\alpha^2\beta N^*P^*}{(a + bN^*)^3}, \end{aligned} \tag{19}$$

we find

$$\omega_{\pm}(E_2) = \sqrt{\frac{-(a_1^2 - a_2^2 - 2a_3) \pm \sqrt{(a_1^2 - a_2^2 - 2a_3)^2 - 4a_3^2}}{2}}, \tag{20}$$

if the conditions  $a_1^2 - a_2^2 - 2a_3 < 0$  and  $(a_1^2 - a_2^2 - 2a_3)^2 - 4a_3^2 > 0$  are satisfied,

$$\tau_n^{\pm}(E_2) = \frac{1}{\omega_{\pm}} \arccos \left( -\frac{a_1}{a_2} \right) + \frac{2n\pi}{\omega_{\pm}}, n = 0, 1, 2, 3, \dots \tag{21}$$

Here, we obtain separate set of values  $\omega_{\pm}(E_2)$  and  $\tau_n^{\pm}(E_2)$  based on the harvesting effort level  $E_2$ . Now the impact of predator harvesting is considered in two separate cases.

**Case 1: When stability switching does not happen in unharvested system**

In this case, if the delayed, unharvested system experiences instability, the system cannot regain its stability for increasing delay. In other words, there exists a  $\tau_0^+(0)$ , such that system remains stable for  $\tau < \tau_0^+(0)$  and unstable for  $\tau > \tau_0^+(0)$  through a Hopf-bifurcation at  $\tau = \tau_0^+(0)$ . We observe from Fig. 4 that the curve  $\tau = \tau_0^+(E_2)$  decreases for coexisting effort range.

For the parameter set as in example 2.1, it results as  $\tau_0^+(0) < \tau_1^+(0) < \tau_0^-(0)$ . The coexisting equilibrium exists in the harvesting effort range  $(0, 0.06)$ . The blue curve in Fig. 4 represents  $\tau = \tau_0^+(E_2)$ , which decreases with the increasing harvesting effort. The black curves represent  $\tau = \tau_{max}$  and  $\tau = \tau_0^+(0)$ , where  $\tau_{max} = \lim_{E_2 \rightarrow 0.06} \tau_0^+(E_2)$ . The region between  $E_2$ - axis and  $\tau = \tau_0^+(E_2)$  is stable, and the region exceeding upward after  $\tau = \tau_0^+(E_2)$  is unstable.

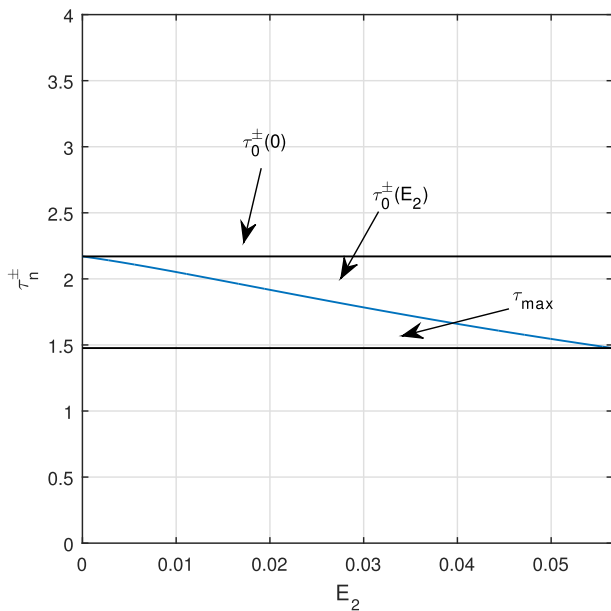


**Fig. 4** Stability and instability region separated by the curve  $\tau = \tau_0^+(E_2)$ . Stable to unstable change is shown with increasing effort

The simulated results on the above example are discussed below based on the range of  $T$ .

(a) If delay  $T$  exists in the region  $(0, \tau_{max})$ , the co-ordinate  $(E_2, T)$  lies in the stability region for all harvesting effort, as shown in Fig. 4. Hence harvesting can not destabilize the system.

(b) If delay  $T \in (\tau_{max}, \tau_0^+(0))$ , the co-ordinate  $(E_2, T)$  lies in a stable region for a small harvesting effort. But with the increased effort, it will enter the unstable region. Thus, a stable unharvested system forever moves to an unstable region with increasing harvesting effort.

(c) If delay  $T > \tau_0^+(0)$ , the co-ordinate  $(E_2, T)$  will always remain in unstable region. Hence, forever instability will occur in this region with increasing effort.

The above analysis shows that we cannot stabilize the system when the unharvested system is in an unstable mode. Unlike in the case of prey harvesting in Fig. 1, where an unstable system can be stabilized, predator harvesting shows destabilizing effects.

**Case II: When the unharvested system shows the stability switching**

Now we intend to study the harvesting effect in the case when an unharvested system shows stability switching. Considering the same set of parameters as in example 2.2 for unharvested system (1), five stability switchings are observed due to delay. For harvested system, the harvesting effort  $E_2$  must lie in the range  $(0, 0.10)$  for coexisting equilibrium. The solid and dashed curves represent  $\tau = \tau_n^+(E_2)$  and  $\tau = \tau_n^-(E_2)$ ,  $(n = 0, 1, 2, \dots)$ , respectively, for increasing harvesting effort (see Fig. 5). The region  $S_1$  enclosed by

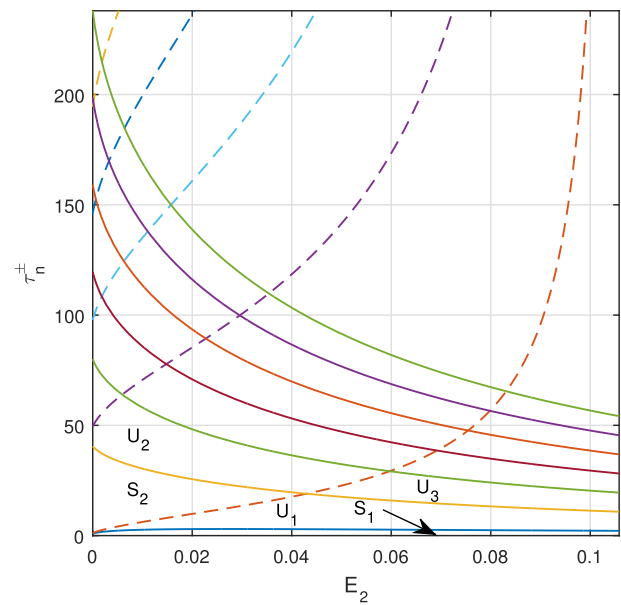


**Fig. 5** Only the curve  $\tau = \tau_0^+(E_2)$  increases up to certain  $E_2$  and then decreases, and the curve  $\tau = \tau_n^+(E_2)$ ,  $n > 0$  (solid) is decreasing and  $\tau = \tau_n^-(E_2)$ ,  $n \geq 0$  (dashed) is increasing with increasing effort and stability switching occurs

$E_2$ -axis and the solid blue curve  $\tau = \tau_0^+(E_2)$  is the stable region for all harvesting effort. The region covered by any solid curve and succeeding dashed curve is the region of instability. The region covered by the dashed curve and succeeding solid curve is the stable region till they intersect with increasing effort. After the intersection of two curves, there simultaneously present two solid curves. This successive presence of two solid curves is the instability region between the curves and regions above the curve for increasing effort  $E_2$ . The explicit discussion follows in Figs. 5 and 6.

In Fig. 5 the closed regions  $S_1, U_1, S_2, U_2, U_3$  are defined as follows.

(a)  $S_1$  is the stable region enclosed by  $E_2$ -axis and  $\tau = \tau_0^+(E_2)$ . (b)  $U_1$  is the unstable region between  $\tau = \tau_0^+(E_2)$  and  $\tau = \tau_0^-(E_2)$ . (c)  $S_2$  is the stable region enclosed by  $\tau = \tau_0^-(E_2)$  and  $\tau = \tau_1^+(E_2)$  up to crossing each other. (d)  $U_3$  is the region of instability as it is the region above the crossing of curves  $\tau = \tau_0^-(E_2)$  and  $\tau = \tau_1^+(E_2)$ . (e)  $U_2$  is the unstable region enclosed by  $\tau = \tau_1^+(E_2), \tau = \tau_0^-(E_2), \tau = \tau_2^+(E_2)$ , and  $\tau = \tau_1^-(E_2)$ .

In Fig. 6 the closed regions  $S_{21}, U_{11}, S_{22}, U_{12}, S_{12}$  are defined as follows. (a)  $S_{21}$  is the stable region enclosed by  $\tau_n^\pm$ -axis,  $\tau = \tau_0^+(E_2)$ , and  $\tau = \tau_{max}$ . (b)  $U_{11}$  is the unstable region enclosed by  $\tau_n^\pm$ -axis,  $\tau = \tau_0^+(E_2)$ ,  $\tau = \tau_0^-(E_2)$ , and  $\tau = \tau_{max}$ . (c)  $S_{22}$  is the stable region enclosed by  $\tau_0^\pm$ -axis,  $\tau = \tau_0^+(E_2)$ ,  $\tau = \tau_{max}$ , and  $\tau = \tau_{peak}$ . (d)  $U_{12}$  is the unstable region enclosed by  $\tau = \tau_0^+$ -axis,  $\tau = \tau_0^-(E_2)$ ,  $\tau = \tau_{max}$ , and  $\tau = \tau_{peak}$ . (e)  $S_{12}$  is the stable region enclosed

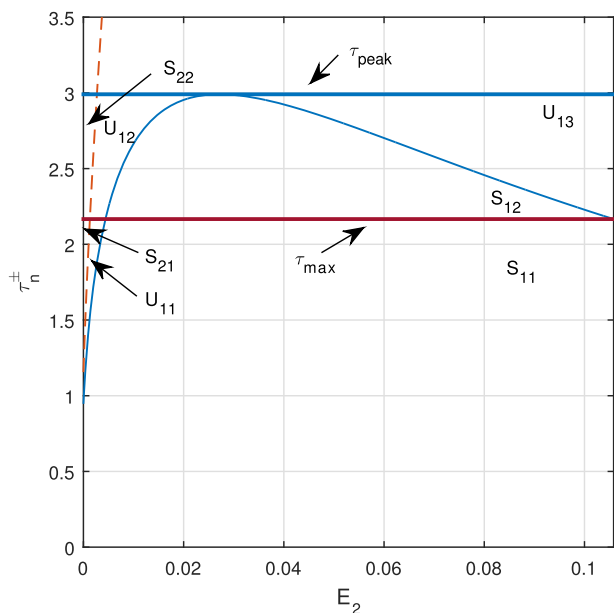


**Fig. 6** The curve  $\tau = \tau_0^+(E_2)$  increases up to  $\tau_{peak}$  and decreases up to  $\tau_{max}$  with increasing effort. The different harvesting effort induces switching of stability

by  $\tau = \tau_0^+(E_2)$  and  $\tau = \tau_{max}$ ;  $U_{13}$  is the unstable region enclosed by  $\tau = \tau_0^+(E_2)$  and  $\tau = \tau_{peak}$ .

Now we observe in Fig. 6 that if the delay  $T \in (0, \tau_0^+(0))$ , the system always experiences stable behavior, which is also observed in the previous case of predator harvesting (see Fig. 4).

Harvesting-induced stability switching may be described as follows:

(a) If delay  $T \in (\tau_0^-(0), \tau_{max})$ , where  $\tau_{max} = \lim_{E_2 \rightarrow 0.10} \tau_0^+(E_2)$ , the co-ordinate  $(E_2, T)$  moves from stable region  $S_{21}$  to unstable region  $U_{11}$  with increasing effort; further, increase of effort enters to stable region  $S_{11}$ . So, a switching of stability occurs for effort increasing (see Fig. 6).

(b) If delay  $T \in (\tau_{max}, \tau_{peak})$ , where  $\tau_{peak} = \max(\tau_0^+(E_2))$ , the co-ordinate  $(E_2, T)$  moves from stable region  $S_{22}$  to unstable region  $U_{12}$  for a small increase of effort. Then, it enters a stable region  $S_{12}$  for further increase of effort. So, stability switching occurs for a certain value of  $E_2$  between the maximum effort. Again if effort increases the co-ordinate fall on unstable region  $U_{13}$ , also a unstable switching  $U_{12}$  to  $S_{12}$  to  $U_{13}$  occurs. In this effort, the range system becomes unstable with the combination of stable and unstable switching with increasing harvesting effort (see Fig. 6).

**2.2.4 Influence of Allee threshold on predator harvesting**

Like prey harvesting, as mentioned earlier, the Allee effect has an important role in dynamics, making the model more sensitive and accurate to understand the dynamical configu-

ration much better for predator harvesting. In the analytical approach to local stability, all the conditions are functions of the Allee threshold for predator harvesting. We are considering the same parameter set as in example 2.2 and observe dynamical changes with the Allee threshold  $k_2 = 0.001, 1, 3, 4, 5, 5.5$ . We obtain the same length of harvesting effort as the co-existing equilibrium exists for harvesting effort  $E_2 \in (0, \frac{k_1\alpha\beta}{a+bk_1} - m)$ , independent of  $k_2$ . Also, obtain the same set of switching times for the pre-harvested system discussed in the influence of prey harvesting. For the pre-harvested system, all  $\tau_n^\pm$  start from the same position.

Here we get the harvesting effort  $E_2 \in (0, 0.10)$ . All the curves  $\tau = \tau_n^+(E_2), n \in \mathbb{N}$  (see Fig. 7) decrease, while the curve  $\tau = \tau_0^+(E_2)$  first increases up to certain level of effort  $E_2$  and then decreases with further increase of effort. Also the curves  $\tau = \tau_n^-(E_2), n \in \mathbb{N} \cup \{0\}$  (see Fig. 7) increase for increasing harvesting effort. For  $k_2 = 0.001, 1, 3, 4, 5, 5.5$ , we get different number of switching 2, 2, 3, 3, 5, 8 respectively in Fig. 7 respectively. But when  $k_2$  increases with increasing harvesting effort, we observe that region of traps between  $\tau = \tau_n^-(E_2), n \in \mathbb{N} \cup \{0\}$  and  $\tau = \tau_n^+(E_2), n \in \mathbb{N}$  decreases. When the Allee threshold is closer to the origin, the area of the region between  $E_2$ - axis and curve  $\tau = \tau_0^+(E_2)$  increases in Fig. 7. Also, when the Allee threshold  $k_2$  increases, the switching number increases, and the system becomes more sensitive. Thus increasing the Allee threshold makes the sensitivity of the system of predator harvesting very high rather than prey harvesting. However, the trapping region is closer to the  $\tau_n^\pm$  axis for increasing the threshold. So in the case of predator harvesting, the whole switching region is significantly less compared to prey harvesting when  $k_2$  increases. Hence for increasing  $k_2$ , the system always moves to the instability region very fast.

**2.2.5 Maximum sustainable yield**

MSY is a maximum sustainable level of yield and exceeds of which reduces population level and ultimately population goes to extinction. The existence of MSY is possible when the equilibrium point is a function of effort as  $N^* = N^*(E_1)$  for prey harvesting and  $P^* = P^*(E_2)$  for predator harvesting. However, in the case of prey harvesting,  $N^*$  is not a function of  $E_1$ . Hence MSY does not exist for prey harvesting. Only predator MSY is possible. In this section, we study the impact of MSY policy on the system due to predator harvesting.

For interior steady state of system (17), the effort  $E_2$  must lie in the range  $(0, \frac{k_1\alpha\beta}{a+bk_1} - m)$ .

The yield at that equilibrium is:

$$y(E_2) = E_2 P^* = E_2 \frac{\left(a + b \frac{(m+E_2)a}{\alpha\beta - (m+E_2)b}\right)}{\alpha}$$

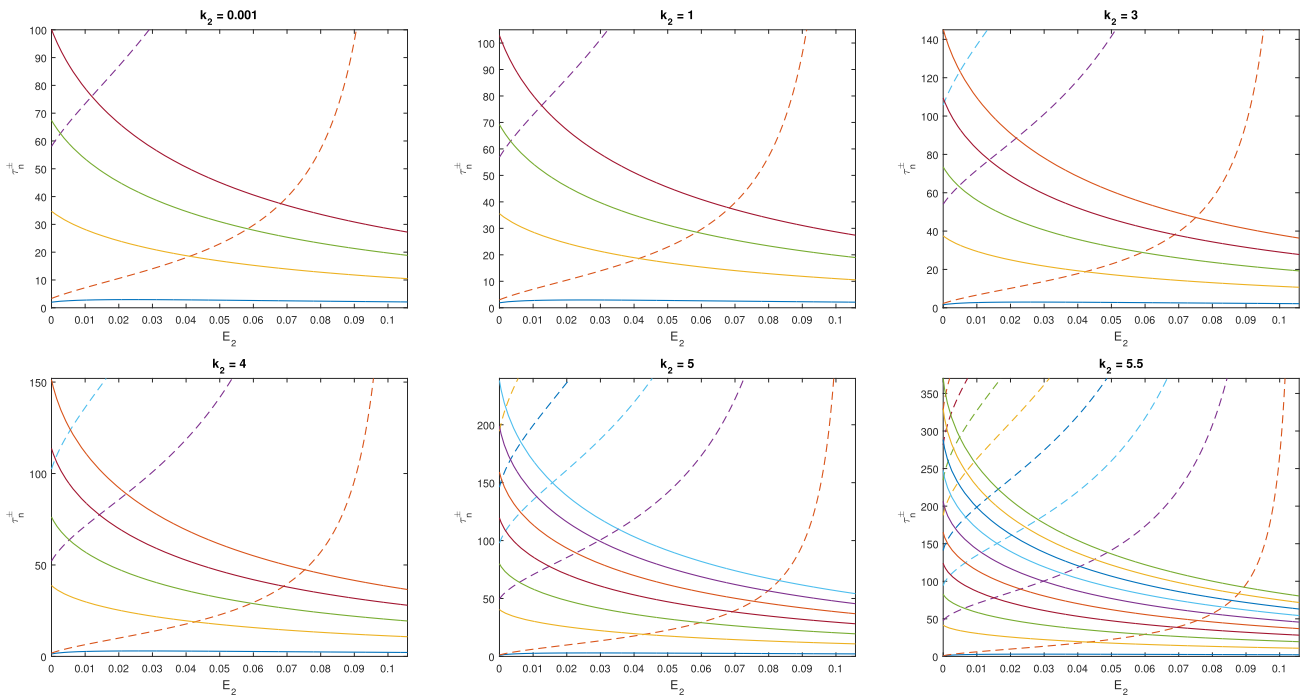


**Fig. 7** Impacts of Allee threshold  $k_2$  on stability switching for  $k_2 = 0.001, 1, 3, 4, 5, 5.5$

$$\left( \frac{r}{k_1} \left( k_1 - \frac{(m + E_2)a}{\alpha\beta - (m + E_2)b} \right) \left( \frac{(m + E_2)a}{\alpha\beta - (m + E_2)b} - k_2 \right) \right).$$

We determine the  $E_2^{MSY}$  for which both the species coexist. The main goal is to determine whether the system's dynamics will be stable in  $(0, E_2^{MSY})$  or not. We plot a vertical line with numeric value  $E_2^{MSY} = 0.03$  in  $E_2 - \tau^\pm$  plane along the curve  $\tau = \tau_0^+(E_2)$ .

The line  $E_2^{MSY} = 0.03$  and curve  $\tau = \tau_0^+(E_2)$  intersect at  $(E_2^{MSY}, \tau^*)$  as shown in Fig. 8. The stability phenomenon is discussed as follows:

- (i) If delay  $T < \tau^*$  in an unharvested system, then positive equilibrium will be stable. For such a case, harvesting at MSY produces a stable stock.
- (ii) If delay  $T$  lies in the range  $(\tau^*, \tau_0^+(0))$  in the unharvested system, then the positive equilibrium is stable also. In such a case, harvesting at MSY does not produce a stable stock.
- (iii) If delay  $T > \tau_0^+(0)$  in the unharvested system, the positive steady state will be in an unstable region, and the equilibrium stock toward the MSY level will be unstable.

So, we cannot assert that the system will sustain stable behavior toward the maximum yield when the pre-harvested system is stable. In other words, MSY does not exist stable state when the pre-harvested system is unstable. The same kind of scenario happens when we treat a more complex parametric situation corresponding to Fig. 6. Although, for a more complex case, we show that predator harvesting at MSY moves into stability whenever the pre-harvested system

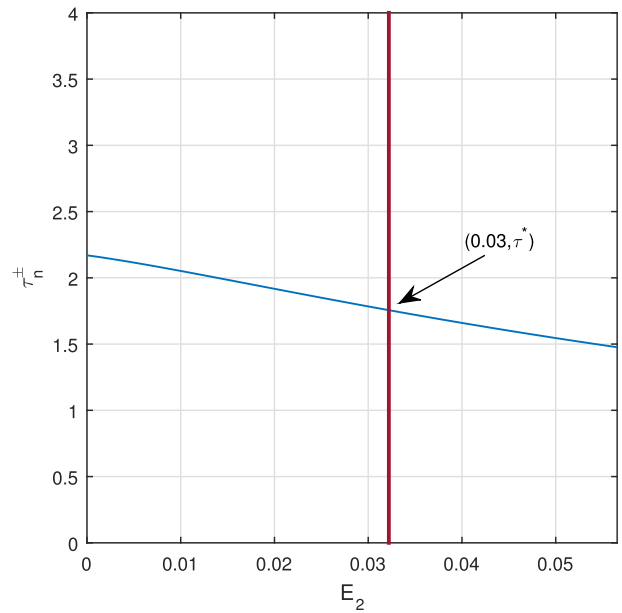


**Fig. 8** The solid blue curve represents  $\tau = \tau_0^+(E_2)$ , and the red vertical line represents  $E_2 = E_2^{MSY}$ . The below portion of curve  $\tau = \tau_0^+(E_2)$  is the stability region. It shows that system may lose stability at the MSY level

experiences unstable behavior. Here the yield is at  $E_2^{MSY} = 0.06$ . If the delay  $T$  lies in the range  $(\tau_0^+(0), \tau_0^-(0))$ , then the system moves from unstable region to stable region up to stable stock. Also one interesting result observed here is that, if delay  $T$  lies in  $(\tau_0^-(0), \tau_{max})$ , the co-ordinate  $(E_2, T)$

moves from the stable region  $S_{21}$  to unstable region  $U_{11}$  and again reaches to stable region  $S_{11}$  up to  $E_2^{MSY}$  for employing effort. If delay  $T$  is in the range  $(\tau_{max}, \tau_{peak})$  then the coordinate  $(E_2, T)$  moves from stable region  $S_{22}$  to unstable region  $U_{21}$  and ultimately reaches to stable region if  $T < \tau^*$ , but for  $T > \tau^*$  will be unstable stock.

### 3 Discussion and conclusion

In this study, we investigate the explicit impact of harvesting on a delayed predator–prey model with the Allee effect. First, we study the dynamics of unexploited system (1). The delay parameter  $\tau$  is taken to investigate the impacts on the stability of system (1). Subsequently, we study the dynamics of the delay model with individual harvesting, namely systems (12) and (17). Two classic properties of real-life populations are the Allee effect and time delay. Most of the theoretical studies were done using instantaneous non-delayed models [25, 64] neglecting the interplay between the time delay and the Allee effect which is poorly understood. In our research, we found that the interplay between the Allee effect and time delay can result in complex dynamics. Here we have explored how the interplay between the effects of delay and the Allee effect can shape the population dynamics in a predator–prey system with harvesting. Our model shows that prey exploitation has different influences depending on the delay-induced dynamics mode for the pre-harvested system. Some explicit impacts are as follows.

- i In case of smaller time delay, when the pre-harvested system is stable, harvesting cannot destabilize the system.
- ii In case of a moderate time delay, when the pre-harvested system is unstable, a significant harvesting effort may stabilize the system.
- iii In case of a higher time delay when the pre-harvested system is unstable, the harvesting effort may not stabilize the system.
- iv In case of fixed time delay, when the pre-harvested system is stable, harvesting can induce stability switching.
- v In case of fixed time delay, when the pre-harvested system is unstable, harvesting can induce instability switching.

Some explicit impacts of predator exploitation on the delay-induced dynamic mode of the pre-harvested system are as follows.

- i In case of a smaller time delay, when the pre-harvested system is stable, predator harvesting may not change the stability as for prey harvesting case.
- ii In the case of the moderate time delay, when the pre-harvested system is stable, an increasing effort may

destabilize the system. In the case of prey harvesting, such a result does not occur.

- iii In case of a significant time delay when the pre-harvested system is unstable, then harvesting may not stabilize the system.
- iv Similar to prey harvesting, predator harvesting also produces stability switching.
- v In case of fixed time delay, when the pre-harvested system is stable, harvesting can induce stability switching as well as instability switching.

It is observed that prey and predator harvesting has distinct impacts on the system.

Another important observation of prey and predator harvesting is in different dynamical changes with delay-induced switching for different Allee thresholds. In both cases, the delay-induced switching region increases with increasing the Allee threshold. However, the prey harvesting region is more significant than predator harvesting. So for a high threshold, little change in predator harvesting range makes the system unstable. Nevertheless, in the case of prey exploitation, the system always becomes unstable after a specific range of harvesting.

Also, we studied the MSY in the presence of the Allee effect and delay for the non-equilibrium steady state due to predator harvesting. We observe the following results.

- i In case of smaller time delay, when the pre-harvested system is stable, then the system moves to stable stock at MSY level.
- ii In case of a larger time delay, the system may not yield stable stock toward MSY, while the pre-harvested system is stable (see Figs. 6 and 8).
- iii In case of a larger time delay, the system may yield unstable stock toward MSY, while the pre-harvested system is unstable (see Fig. 6).
- iv In case of a more significant time delay, the system may yield stable stock at MSY by an intermediate stable switching, while the pre-harvested system is stable (see Fig. 6).
- v In case of more considerable time delay, the system may yield unstable stock at MSY by an intermediate stable and unstable switching (see Fig. 6).

The future perspectives of our research may extend to the reaction-diffusion phenomenon and stochasticity with random parameters and a fractional approach. Also, we can use the fear effect and different functional responses.

**Acknowledgements** We acknowledge the anonymous reviewers for their comments which improves the quality of the paper. We would also like to thank the Editor-in-Chief, Jian-Qiao Sun, for providing an opportunity for possible publication in the journal.

**Author Contributions** The whole manuscript is made by Bidhan Bhunia, T.K.Kar, and Papiya Debnath. Bidhan Bhunia and T.K.Kar have an important role in designing the approach, model analysis, and manuscript writing, with substantial input from Papiya Debnath.

**Data availability** No data applicable.

## Declarations

**Funding** Bidhan Bhunia expresses gratefulness to UGC-NFSC (Ref. No. 191620076432), Government of India, for financial support in pursuing his PhD. The research of Tapan Kumar Kar is partially supported by the Council of Scientific and Industrial Research (CSIR), India (No. 25(0300)/19/EMR-II, dated: May 16, 2019).

**Conflict of interest** The authors declare that they have no conflict of interest regarding this work.

## References

- Beddington JR, May RM (1980) Maximum sustainable yields in systems subject to harvesting at more than one trophic level. *Math Biosci* 51(3–4):261–281. [https://doi.org/10.1016/0025-5564\(80\)90103-0](https://doi.org/10.1016/0025-5564(80)90103-0)
- Schaefer MB (1954) Some aspects of the dynamics of populations important to the management of the commercial marine fisheries. *Int Am Trop Tuna Com Bull* 1(2):23–56
- May RM, Beddington JR, Clark CW, Holt SJ, Laws RM (1979) Management of multispecies fisheries. *Science* 205(4403):267–277. <https://doi.org/10.1126/science.205.4403.267>
- Ghosh B, Pal D, Kar TK, Valverde JC (2017) Biological conservation through marine protected areas in the presence of alternative stable states. *Math Biosci* 286:49–57. <https://doi.org/10.1016/j.mbs.2017.02.004>
- Kar TK, Ghosh B (2013) Sustainability and economic consequences of creating marine protected areas in multispecies multi-activity context. *J Theor Biol* 318:81–90. <https://doi.org/10.1016/j.jtbi.2012.11.004>
- Tromeur E, Luc D (2016) Optimal biodiversity erosion in multispecies fisheries. *Les Cahiers du GREThA-Groupe de Recherche en éorrique et Appliquée*, Bordeaux
- Pikitch EK, Santora C, Babcock EA, Bakun A, Bonfil R, Conover DO, Dayton P, Doukakis P, Fluharty D, Heneman B, Houde ED (2004) Ecosystem-based fishery management. *Science* 305(5682):346–347. <https://doi.org/10.1126/science.1098222>
- Tromeur E, Loeuille N (2017) Balancing yield with resilience and conservation objectives in harvested predator-prey communities. *Oikos* 126(12):1780–1789. <https://doi.org/10.1111/oik.03985>
- Pujaru K, Kar TK (2020) Impacts of predator-prey interaction on managing maximum sustainable yield and resilience. *Nonlinear Anal Model Control* 25(3):400–416. <https://doi.org/10.15388/namc.2020.25.16657>
- Hilborn R (2010) Pretty good yield and exploited fishes. *Mar Policy* 34(1):193–196. <https://doi.org/10.1016/j.marpol.2009.04.013>
- Dunn RP, Baskett ML, Hovel KA (2017) Interactive effects of predator and prey harvest on ecological resilience of rocky reefs. *Ecol Appl* 27(6):1718–1730. <https://doi.org/10.1002/eap.1581>
- Geček S, Legović T (2012) Impact of maximum sustainable yield on competitive community. *J Theor Biol* 307:96–103. <https://doi.org/10.1016/j.jtbi.2012.04.027>
- Ghosh B, Kar TK, Legović T (2014) Sustainability of exploited ecologically interdependent species. *Popul Ecol* 56(3):527–537
- Legović T (2008) Impact of demersal fishery and evidence of the Volterra principle to the extreme in the Adriatic sea. *Ecol Model* 212(1–2):68–73. <https://doi.org/10.1016/j.ecolmodel.2007.10.014>
- Matsuda H, Abrams PA (2006) Maximal yields from multispecies fisheries systems: rules for systems with multiple trophic levels. *Ecological Applications* 16(1):225–237. <https://doi.org/10.1890/05-0346>
- Abrams PA, Roth JD (1994) The effects of enrichment of three-species food chains with nonlinear functional responses. *Ecology* 75(4):1118–1130. <https://doi.org/10.2307/1939435>
- Hastings A, Powell T (1991) Chaos in a three-species food chain. *Ecology* 72(3):896–903. <https://doi.org/10.2307/1940591>
- Klebanoff A, Hastings A (1994) Chaos in one-predator, two-prey models: cgeneral results from bifurcation theory. *Math Biosci* 122(2):221–233. [https://doi.org/10.1016/0025-5564\(94\)90059-0](https://doi.org/10.1016/0025-5564(94)90059-0)
- Ghosh B, Kar TK, Legović T (2014) Relationship between exploitation, oscillation, MSY and extinction. *Math Biosci* 256:1–9. <https://doi.org/10.1016/j.mbs.2014.07.005>
- Ghosh B, Pal D, Legović T, Kar TK (2018) Harvesting induced stability and instability in a tri-trophic food chain. *Math Biosci* 304:89–99. <https://doi.org/10.1016/j.mbs.2018.08.003>
- Hadjiavgousti D, Ichtiaroglou S (2008) Allee effect in a prey-predator system. *Chaos Solitons Fractals* 36(2):334–342. <https://doi.org/10.1016/j.chaos.2006.06.053>
- Stephens PA, Sutherland WJ (1999) Consequences of the Allee effect for behaviour, ecology and conservation. *Trends in Ecol Evol* 14(10):401–405. [https://doi.org/10.1016/S0169-5347\(99\)01684-5](https://doi.org/10.1016/S0169-5347(99)01684-5)
- Zhou SR, Liu YF, Wang G (2005) The stability of predator-prey systems subject to the Allee effects. *Theor Popul Biol* 67(1):23–31. <https://doi.org/10.1016/j.tpb.2004.06.007>
- Wang G, Liang XG, Wang FZ (1999) The competitive dynamics of populations subject to an Allee effect. *Ecol Model* 124(2–3):183–192. [https://doi.org/10.1016/S0304-3800\(99\)00160-X](https://doi.org/10.1016/S0304-3800(99)00160-X)
- Zu J, Mimura M (2010) The impact of Allee effect on a predator-prey system with Holling type II functional response. *Appl Math Comput* 217(7):3542–3556. <https://doi.org/10.1016/j.amc.2010.09.029>
- Çelik C, Merdan H, Duman O, Akin Ö (2008) Allee effects on population dynamics with delay. *Chaos Solitons Fractals* 37(1):65–74. <https://doi.org/10.1016/j.chaos.2006.08.019>
- Fowler MS, Ruxton GD (2002) Population dynamic consequences of Allee effects. *J Theor Biol* 215(1):39–46. <https://doi.org/10.1006/jtbi.2001.2486>
- Jang SJ (2007) Allee effects in a discrete-time host-parasitoid model with stage structure in the host. *Discret Contin Dyn Syst B* 8(1):145. <https://doi.org/10.3934/dcdsb.2007.8.145>
- López-Ruiz R, Fournier-Prunaret D (2005) Indirect Allee effect, bistability and chaotic oscillations in a predator-prey discrete model of logistic type. *Chaos Solitons Fractals* 24(1):85–101. <https://doi.org/10.1016/j.chaos.2004.07.018>
- McCarthy MA (1997) The Allee effect, finding mates and theoretical models. *Ecol Model* 103(1):99–102
- Merdan H, Duman O (2009) On the stability analysis of a general discrete-time population model involving predation and Allee effects. *Chaos Solitons Fractals* 40(3):1169–1175. <https://doi.org/10.1016/j.chaos.2007.08.081>
- Merdan H, Duman O, Akin Ö, Çelik C (2009) Allee effects on population dynamics in continuous (overlapping) case. *Chaos Solitons Fractals* 39(4):1994–2001. <https://doi.org/10.1016/j.chaos.2007.06.062>
- González-Olivares E, Meneses-Alcay H, Gonzalez-Yanez B, Mena-Lorca J, Rojas-Palma A, Ramos-Jiliberto R (2011) Multiple stability and uniqueness of the limit cycle in a Gause-type predator-prey model considering the Allee effect on prey. *Non-*

- linear Anal Real World Appl 12(6):2931–2942. <https://doi.org/10.1016/j.nonrwa.2011.04.003>
34. Duman O, Merdan H (2009) Stability analysis of continuous population model involving predation and Allee effect. *Chaos Solitons Fractals* 41(3):1218–1222. <https://doi.org/10.1016/j.chaos.2008.05.008>
  35. Merdan H (2010) Stability analysis of a Lotka-Volterra type predator-prey system involving Allee effects. *Anziam J* 52(2):139–145. <https://doi.org/10.1017/S1446181111000630>
  36. Berec L, Angulo E, Courchamp F (2007) Multiple Allee effects and population management. *Trends Ecol Evol* 22(4):185–191. <https://doi.org/10.1016/j.tree.2006.12.002>
  37. Freedman HI, Gopalsamy K (1986) Global stability in time-delayed single-species dynamics. *Bull Math Biol* 48(5):485–492
  38. Nicholson AJ (1954) An outline of the dynamics of animal populations. *Aust J Zool* 2(1):9–65. <https://doi.org/10.1071/ZO9540009>
  39. Hutchinson GE (1948) Circular causal systems in ecology. *Ann N Y Acad Sci* 50(4):221–246
  40. Rihan FA, Lakshmanan S, Hashish AH, Rakkiyappan R, Ahmed E (2015) Fractional-order delayed predator-prey systems with Holling type-II functional response. *Nonlinear Dyn* 80(1):777–789
  41. Batzel JJ, Tran HT (2000) Stability of the human respiratory control system I. Analysis of a two-dimensional delay state-space model. *J Math Biol* 41(1):45–79
  42. Bocharov GA, Rihan FA (2000) Numerical modelling in biosciences using delay differential equations. *J Comput Appl Math* 125(1–2):183–199. [https://doi.org/10.1016/S0377-0427\(00\)00468-4](https://doi.org/10.1016/S0377-0427(00)00468-4)
  43. Rihan FA, Azamov AA, Al-Sakaji HJ (2018) An inverse problem for delay differential equations: parameter estimation, nonlinearity, sensitivity. *Appl Math Inf Sci* 12(1):63–74. <https://doi.org/10.18576/amis/120106>
  44. Banerjee M, Takeuchi Y (2017) Maturation delay for the predators can enhance stable coexistence for a class of prey-predator models. *J Theor Biol* 412:154–171. <https://doi.org/10.1016/j.jtbi.2016.10.016>
  45. Chen YM, Zhang FQ (2013) Dynamics of a delayed predator-prey model with predator migration. *Appl Math Model* 37(3):1400–1412. <https://doi.org/10.1016/j.apm.2012.04.012>
  46. Li H, Meng G, She Z (2016) Stability and Hopf bifurcation of a delayed density-dependent predator-prey system with Beddington-DeAngelis functional response. *Int J Bifurc Chaos* 26(10):1650165. <https://doi.org/10.1142/S0218127416501650>
  47. Wang X, Zou X (2017) Modeling the fear effect in predator-prey interactions with adaptive avoidance of predators. *Bull Math Biol* 79(6):1325–1359
  48. Zhang H, Xia J, Georgescu P (2017) Multigroup deterministic and stochastic SEIR epidemic models with nonlinear incidence rates and distributed delays: a stability analysis. *Math Methods Appl Sci* 40(18):6254–6275. <https://doi.org/10.1002/mma.4453>
  49. Zhang H, Xia J, Georgescu P (2017) Stability analyses of deterministic and stochastic SEIR epidemic models with nonlinear incidence rates and distributed delay. *Nonlinear Anal Model Control* 22(1):64–83. <https://doi.org/10.15388/NA.2017.1.5>
  50. Gourley SA, Kuang YA (2004) stage structured predator-prey model and its dependence on maturation delay and death rate. *J Math Biol* 49(2):188–200
  51. Ho CP, Ou YL (2002) Influence of time delay on local stability for a predator-prey system. *J Tunghai Sci* 4:47–62
  52. Banerjee J, Sasmal SK, Layek RK (2019) Supercritical and subcritical Hopf-bifurcations in a two-delayed prey-predator system with density-dependent mortality of predator and strong Allee effect in prey. *Biosyst* 180:19–37. <https://doi.org/10.1016/j.biosystems.2019.02.011>
  53. Anacleto M, Vidal C (2020) Dynamics of a delayed predator-prey model with Allee effect and Holling type II functional response. *Math Methods Appl Sci* 43(9):5708–5728. <https://doi.org/10.1002/mma.6307>
  54. Huang J, Gong Y, Ruan S (2013) Bifurcation analysis in a predator-prey model with constant-yield predator harvesting. *Discret Contin Dyn Syst B* 18(8):2101–2121. <https://doi.org/10.3934/dcdsb.2013.18.2101>
  55. Xiao D, Jennings LS (2005) Bifurcations of a ratio-dependent predator-prey system with constant rate harvesting. *SIAM Journal on Applied Mathematics* 65(3):737–753. <https://doi.org/10.1137/S0036139903428719>
  56. Kar TK, Chaudhuri KS (2002) On non-selective harvesting of a multispecies fishery. *Int J Math Educ Sci Technol* 33(4):543–556
  57. Kar TK (2003) Selective harvesting in a prey-predator fishery with time delay. *Math Comput Model* 38(3–4):449–458. [https://doi.org/10.1016/S0895-7177\(03\)90099-9](https://doi.org/10.1016/S0895-7177(03)90099-9)
  58. Kar TK, Ghorai A (2011) Dynamic behavior of a delayed predator-prey model with harvesting. *Appl Math Comput* 217(22):9085–9104. <https://doi.org/10.1016/j.amc.2011.03.126>
  59. Liu M, Yu J, Mandal PS (2018) Dynamics of a stochastic delay competitive model with harvesting and Markovian switching. *Appl Math Comput* 337:335–349. <https://doi.org/10.1016/j.amc.2018.03.044>
  60. Kar TK, Pahari UK (2007) Modelling and analysis of a prey-predator system with stage-structure and harvesting. *Nonlinear Anal Real World Appl* 8(2):601–609. <https://doi.org/10.1016/j.nonrwa.2006.01.004>
  61. Martin A, Ruan S (2001) Predator-prey models with delay and prey harvesting. *J Math Biol* 43(3):247–267. <https://doi.org/10.1007/s002850100095>
  62. Barman B, Ghosh B (2019) Explicit impacts of harvesting in delayed predator-prey models. *Chaos Solitons Fractals* 122:213–228. <https://doi.org/10.1016/j.chaos.2019.03.002>
  63. Meng XY, Li J (2020) Stability and Hopf bifurcation analysis of a delayed phytoplankton-zooplankton model with Allee effect and linear harvesting. *Math Biosci Eng* 17(3):1973–2002. <https://doi.org/10.3934/mbe.2020105>
  64. Ma Y, Zhao M, Du Y (2022) Impact of the strong Allee effect in a predator-prey model. *AIMS Math* 7(9):16296–16314. <https://doi.org/10.3934/math.2022890>

Springer Nature or its licensor (e.g. a society or other partner) holds exclusive rights to this article under a publishing agreement with the author(s) or other rightsholder(s); author self-archiving of the accepted manuscript version of this article is solely governed by the terms of such publishing agreement and applicable law.